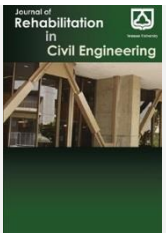

Journal of Rehabilitation in Civil Engineering

Journal homepage: https://civiljournal.semnan.ac.ir/

Structural Damage Detection under Short Time Load Using Cascade-Forward Network

Seyed Sina Kourehli [1,*]

1. Department of Civil Engineering, Azarbaijan Shahid Madani University, Tabriz, Iran

* Corresponding author: *ss.kourehli@azaruniv.ac.ir*

ARTICLE INFO

Article history:
Received: 22 July 2023
Revised: 08 October 2023
Accepted: 31 December 2023

Keywords:
Damage;
Short time load;
State space;
Cascade-forward network.

ABSTRACT

Damage identification in structures is one of the most important problems in structural engineering because early damage detection prevents a catastrophic event in structures. In this paper, a new damage identification method proposed based on a short time load excitement and dynamic time history response of structures as a damage index. To solve the equation of motion of structure, the state space method was used. To identify damage in different structures, cascade-forward network has been used. In the training process of machine, the time history of dynamic responses used as input and damage states as output. The novelty of present method is the application of time history responses of structure under short time loading excitation to train cascade-forward network. To show the efficiency of presented method, three examples consist of a frame, bending plate and beam structures has been investigated. The obtained results reveal that proposed method is viable in detecting damage in different structures.

E-ISSN: 2345-4423

How to cite this article:
Kourehli, S. S. (2024). Structural Damage Detection under Short Time Load Using Cascade-Forward Network. Journal of Rehabilitation in Civil Engineering, 12(3), 32-42. https://doi.org/10.22075/jrce.2023.31320.1885

1. Introduction

In the last decades, the structural damage detection is one the important problems in structural and earthquake engineering fields. To damage detection different methods proposed by researchers. One of these methods is the signal base methods. In this method the measured or calculated dynamic time history responses of structures under different excitation has been used as a damage indicator. I n the recent years many signal based methods proposed. Bagheri and Kourehli [1] presented a time history response-based damage detection method under seismic excitation. In this study, a benchmark problem provided by the IASC-ASCE Task Group on Structural Health Monitoring and a simulated shear wall model investigated under different earthquake accelerations [2,3]. To show the efficiency of this method, wavelet transform used to show time of damage occurrence. Abrupt changes in wavelet coefficient show the occurrence time of damage in structures. In other study, Kourehli [4] used the wavelet transform to identify damage in steel frame's connections. In this study, concentrated springs used to model steel frame connections. The obtained results were acceptable to detect damage in connections. In other work, Jahangir et al. [5] presented a damage detection method in prestressed concrete slabs using wavelet analysis of vibration responses in the time domain. Beheshti Aval et al [6] proposed a signal-based method to identify damage in structure. In this study, seismic structural health monitoring technique presented for damage location and severity identification of a multi-story frame subjected to an earthquake excitation. Also, Roveri and Carcaterra [7] proposed Hilbert–Huang transform to identify damage of bridge structures under a traveling load. In other study, Yin et al. [8] presented a connection damage identification method using incomplete modal data by Bayesian approach and model reduction technique. Also, Kourehli [9] presented a damage identification method using limited number of sensors and extreme learning machine (ELM). To condense mass and stiffness matrices, the second-order approximation of Neumann series expansion (NSEMR-II) has been used. Also, Katkhuda et al. [10] proposed a method that combines the iterative least-square and unscented Kalman filter (UKF) methods to identify the stiffness of beams and columns in typical two-dimensional steel-framed structures with semirigid connections. The detection of damages was done by using a nonlinear time-domain structural health monitoring method. In this study, harmonic and blast loads were used, and structural responses were measured by only a limited number of accelerometer sensors. Zimin and Zimmerman [11] presented a computer-based time domain periodogram analysis algorithm and demonstrate its' utility for determining the existence of structural damage. In other work, Kourehli [12] presented gaussian process regression model for damage localization in plates based on modal data. To show the effectiveness of presented approach, a two-fixed supported plate and a cantilever plate was studied. Also, Seyedpoor et al. [13] presented a damage identification method using the nodal accelerations measured at the limited points of a structure subjected to an impulse load. In this paper an optimization problem solved using differential evolution algorithm (DEA).

In this paper, a new time history response-based damage identification method has been proposed. In most of previous works, the modal data used as a damage indicator; while, in this paper changes in dynamic responses of structures under short time loading excitation has been used. To solve the equation of motion of structures, state space-based method has been used. Three different structures consist of a steel plane frame, concrete bending plate and steel cantilever beam finite element has been modeled in MATLAB environment.

2. Problem formulation

In this section theoretical background of proposed method is presented. First, the formulation of equation of motion under short time load presented. Secondly, the state space method presented as an effective tool to solve the equation of motion under short time load. Finally, to identify damage in studied structures, cascade-forward network (CFN) has been used. In the training process of machine, the time history of dynamic responses used as input and damage states as output.

2.1. Formulation of equation of motion under short time load

In this paper, damage identification has been done using time history responses of structure under short time load. The equation of motion of multi degree of freedoms (MDOF) can be formulated as follows:

$$\mathrm{M}\ddot{\mathrm{X}}(t) + \mathrm{C}\dot{\mathrm{X}}(t) + \mathrm{KX}(t) = \mathrm{F(t)} \quad (1)$$

where, M, C, and K are mass, damping, and stiffness matrices of the structure, respectively; X is the vector of displacements; F(t) is the time history of short time exciting external force.

2.2. State space method

Linearized state equation and output equation can be written as follow:

$$\begin{aligned} \dot{\mathrm{x}}(\mathrm{t}) &= \mathrm{A(t)x(t)} + \mathrm{B(t)u(t)} \\ \mathrm{y(t)} &= \mathrm{C(t)x(t)} + \mathrm{D(t)u(t)} \end{aligned} \quad (2)$$

where *A(t)* is called the state matrix, *B(t)* the input matrix, *C(t)* the output matrix, and *D(t)* the direct transmission matrix [14]. The Block diagram of system in state space presented in Fig. 1.

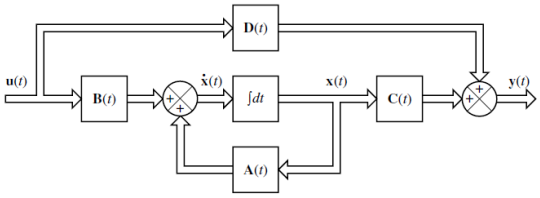

Fig. 1. Block diagram of the linear, continuous time system represented in state space [14].

For a structural system, the state variables are the displacements and velocities. Instead of working with *n* equations of motion for the *n* degrees of freedom, the second order equations have been broken into *2n* first order equations. The equation for the case of multiple degree of freedom is

$$\dot{X} = HX + GF \quad (3)$$

Where the vector *X* is a vector of size *2n* containing the displacement and velocities at the nodes of the structure. It completely defines the state of the system at any time.

$$X = \begin{bmatrix} U \\ \dot{U} \end{bmatrix} \quad (4)$$

H contains the system parameters; *F* contains the external excitation and *G* is called the locator matrix. The vector $\dot{X}$ represents the first order change of the state of the system.

$$\begin{aligned} H &= \begin{bmatrix} 0 & I \\ -M^{-1}K & -M^{-1}C \end{bmatrix}; \\ G &= \begin{bmatrix} 0 \\ M^{-1}E \end{bmatrix} \end{aligned} \quad (5)$$

The *E* matric contains just ones on the places where the forces are located and simply zeros where there are no forces [15].

2.3. Cascade-forward network (CFN)

Cascade-forward networks are similar to feed-forward networks, but include a connection from the input and every previous layer to following layers. As with feed-forward networks, a two-or more layer cascade-network can learn any finite input-output relationship arbitrarily well given enough hidden neurons [16]. The advantage of this method is that it accommodates the nonlinear

relationship between input and output by not eliminating the linear relationship between the two [17].

The Hyperbolic tangent sigmoid transfer function and Linear transfer function are found appropriate for the hidden and output node activation functions, respectively. As for the network, the training function used in the Cascade -forward-back propagation were Levenberg–Marquardt algorithm. Also, MSE (minimum square error) was chosen as the performance function. The ANN was implemented by using MATLAB software [16]. The best configuration for the Cascade-forward network (CFN) is listed in Table 1.

Table 1. Best configuration for the CFN.

Examples	Number of input layer neurons	Number of hidden layer neurons	Number of output layer neurons
Frame	76	30	8
Flexural Plate	76	30	9
Cantilever Beam	76	30	9

3. Examples

To show efficiency of proposed method, three different examples consist of steel plane frame, concrete flexural plate and steel cantilever beam structures has been studied. To train Cascade-forward network (CFN) in different examples, displacement and velocity time history responses in translational degree of freedoms used as input. In frame, plate and beam structures, translational degree of freedoms numbers 7 and 13, 7 and 16, 1 and 17, respectively; between times interval 0.1 and 1.9 seconds (time steps are 0.1 seconds) has been used as input. Damages are considered as element stiffness reductions. In this study, the behavior of structures are linear.

Figure 2 shows the flowchart of the proposed method for damage detection and estimation in structural elements. In this paper, damage is considered as reduction in Young's modulus of finite elements.

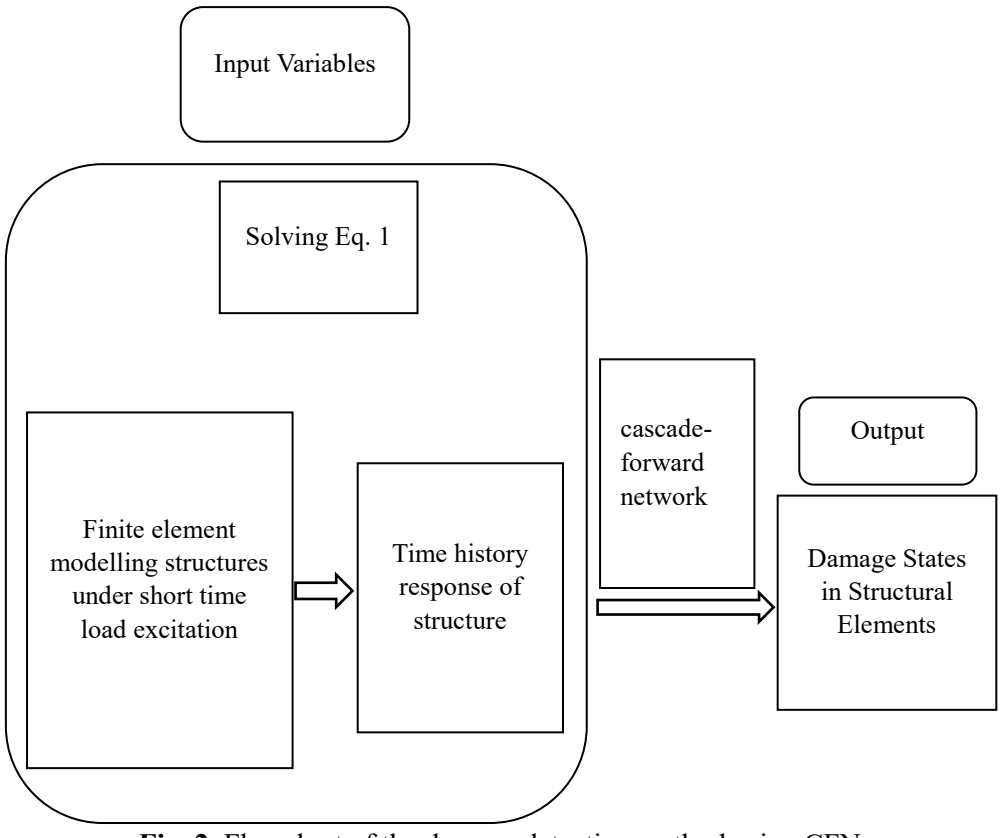

Fig. 2. Flowchart of the damage detection method using CFN.

3.1. Frame structure

A two-story plane frame as illustrated in Fig. 3 with a finite-element model consisting of 8 elements (five columns and three beams), five nodes and fifteen degree of freedoms is considered. The numerical studies are carried out within the MATLAB (2022) environment [16], which is used for the solution of finite element problems. For the steel frame considered, the material properties of the steel include Young's modulus E=200 GPa, mass density ρ=7850 kg/m3. The moment of inertia and cross-sectional area of the columns are: $I=11280\times10^{-8}$ m^4 and $A=106\times10^{-4}$ m^2, respectively; for the beams are: $I=5790\times10^{-8}$ m^4 and $A=45.9\times10^{-4}$ m^2. For this example, ten damage scenarios has been considered as seen in Table 3. As it can be seen from Fig. 3, short time load excitation is applied at DOF=13 where F_0 = 200 kN and T_0 = 0.2 s.

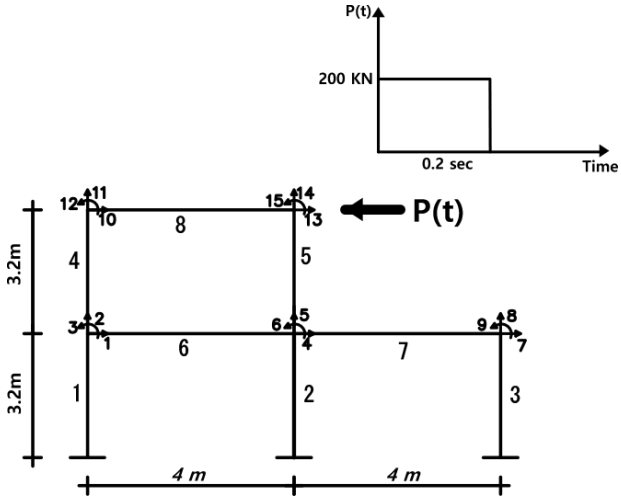

Fig. 3. Finite element model of the two-story plane frame.

The time history displacement and velocity responses of frame structure for ten assigned damage scenarios presented in Fig. 4. It can be seen that the time history displacement and velocity responses change due to the structural damages and sensitive to structural damages and can be used as a damage indicator. In other word, the time history displacement and velocity responses are sensitive damage indicators.

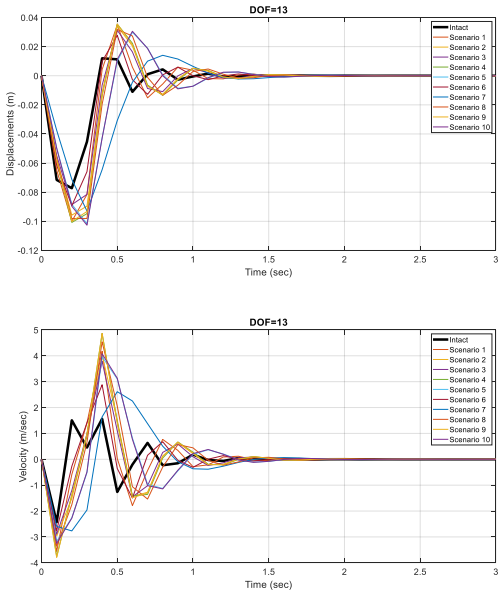

Fig. 4. Time history displacement and velocity responses of frame structure.

For frame structure, the CFN performance in training, validation and testing stages presented in Table 2. Validation is used to measure network generalization, and to halt training when generalization stops improving. Testing has no effect on training and so provides an independent measure of network performance during and after training. The mean-square error (MSE) and Correlation Coefficient (R) of the actual and detected damage severity values are determined. R value of unity means a close relationship and zero a random relationship. The MSE is the average squared difference between the outputs and targets, with lower values on the better side. According to Table 2, R values are near unity and MSE values are near zero that means the CFN trained accurately.

Table 2. Statistics for training, validation and testing for frame.

	Samples	MSE	R
Training	907	18e-5	0.9962
Validation	194	11e-4	0.9829
Testing	194	15.4e-4	0.9723

Finally, to show the performance of presented method in damage identification, ten random damage scenarios generated and damages

detected. Table 3, reveal the efficiency of proposed method in detecting damages in different elements. In other word, the values of detected damages are close to actual damage values which show the accuracy of presented method.

Table 3. The detected damages for ten different scenarios of frame.

Scenario 1		Scenario 2		Scenario 3		Scenario 4		Scenario 5	
Actual	Detected	Actual	Detected	Actual	Detected	Actual	Detected	Actual	Detected
0.2	0.19	0.2	0.20	0.0	0.00	0.0	0.00	0.2	0.19
0.0	0.00	0.4	0.38	0.0	0.00	0.0	0.00	0.4	0.39
0.2	0.20	0.2	0.20	0.2	0.18	0.2	0.19	0.2	0.22
0.2	0.20	0.2	0.18	0.2	0.18	0.0	0.00	0.4	0.41
0.0	0.02	0.2	0.20	0.2	0.21	0.0	0.01	0.2	0.19
0.4	0.39	0.4	0.38	0.0	0.00	0.2	0.21	0.0	0.00
0.0	0.01	0.0	0.02	0.0	0.00	0.0	0.00	0.0	0.00
0.0	0.00	0.2	0.20	0.0	0.00	0.2	0.20	0.2	0.20
Scenario 6		Scenario 7		Scenario 8		Scenario 9		Scenario 10	
Actual	Detected	Actual	Detected	Actual	Detected	Actual	Detected	Actual	Detected
0.0	0.00	0.0	0.05	0.0	0.00	0.2	0.22	0.2	0.21
0.4	0.38	0.2	0.18	0.0	0.00	0.4	0.38	0.0	0.0
0.2	0.21	0.0	0.03	0.0	0.00	0.0	0.01	0.2	0.21
0.0	0.01	0.4	0.36	0.4	0.40	0.0	0.00	0.0	0.00
0.0	0.01	0.0	0.03	0.2	0.20	0.0	0.01	0.0	0.01
0.2	0.20	0.2	0.19	0.4	0.39	0.4	0.41	0.0	0.41
0.0	0.01	0.2	0.22	0.2	0.20	0.2	0.17	0.2	0.2
0.0	0.00	0.0	0.00	0.0	0.00	0.0	0.00	0.4	0.4

3.2. Flexural Plate structure

The second example is a three-fixed supported flexural plate as illustrated in Fig. 5 with finite element model consists of 9 elements and 16 nodes. The thickness of considered concrete plate is t=0.1m and the material properties include Young's modulus of E=20 GPa, mass density of ρ=2400 kg/m^3 and Poisson's ratio of μ=0.2. The short time load excitation is applied at DOF=16 in *z* direction as shown in Figure 2 where F0 = 20 kN and T_0 = 0.2 s. For the flexural plate structure, ten damage scenarios has been considered as seen in Table 5.

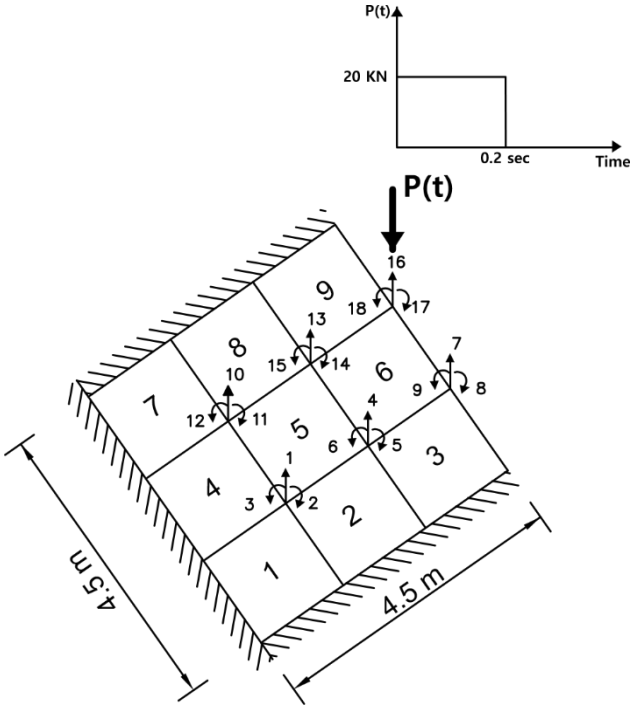

Fig. 5. Finite element model of the flexural plate.

Time history displacement and velocity responses of flexural plate structure as a damage indicator in DOF=7 is shown in Fig. 6 for ten different damage scenarios.

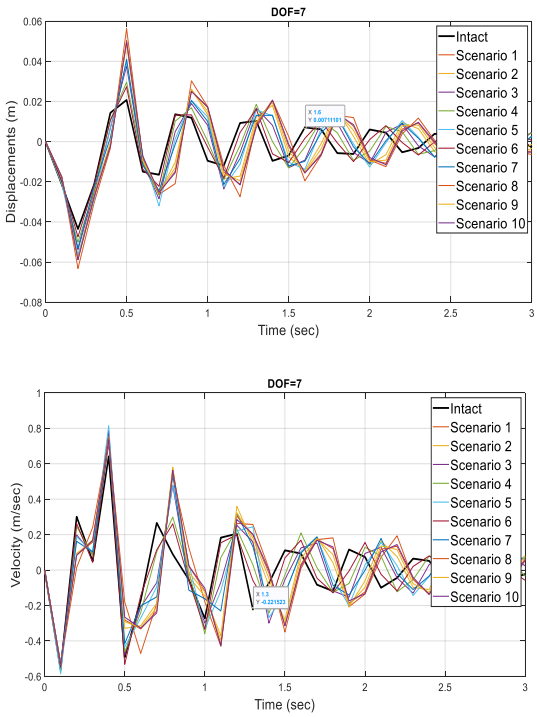

Fig. 6. Time history displacement and velocity responses of plate structure.

It can be seen that these responses are sensitive to structural damages and can be used as a

damage indicator. For plate structure, the time history displacement and velocity responses are sensitive damage indicators. Also, three-dimensional graph of displacement of plate in different time steps during dynamic analysis under short time loading presented in Fig. 7.

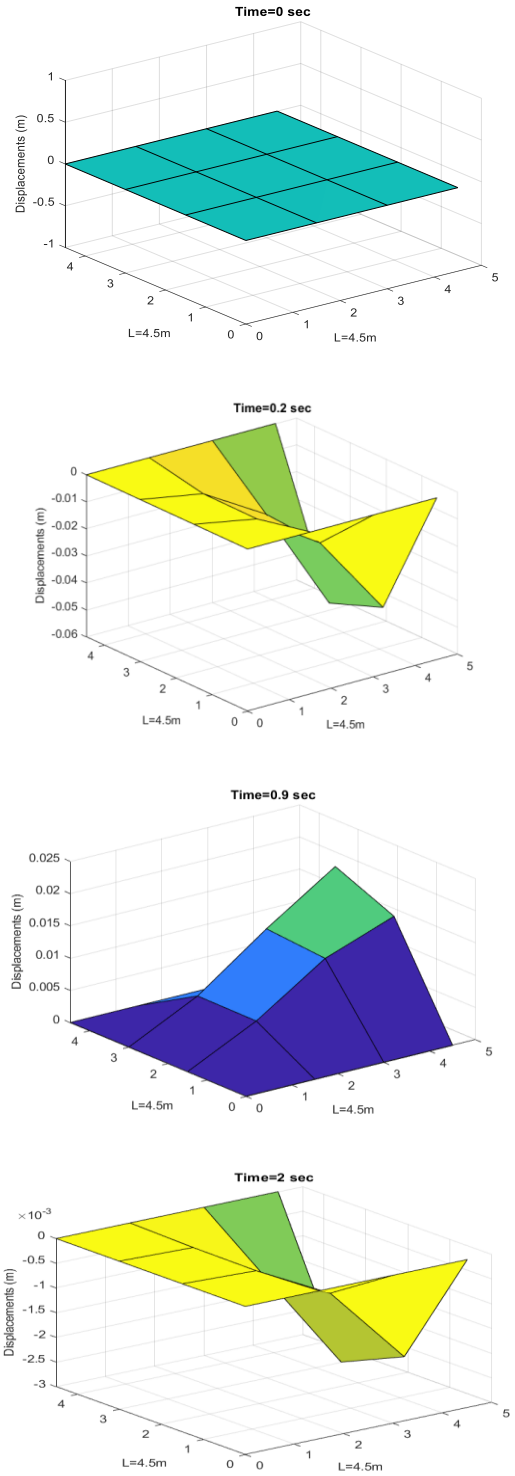

Fig. 7. Displacement of plate in different times during dynamic analysis (Damage in Elements no. 1, 3, 4, 5 is 0.2).

For flexural plate structure, the CFN performance presented in Table 4. According to Table 4, the CFN can be used confidently in training process of bending plate structure.

Table 4. Statistics for training, validation and testing for plate.

	Samples	MSE	R
Training	907	1.2e-7	0.999
Validation	194	1.5e-6	0.999
Testing	194	1.8e-6	0.999

According to Table 5, ten different random damage scenarios has been used to investigate the proposed method performance. It can be seen that the damage severities and locations can detect accurately.

Table 5. The detected damages for ten different scenarios of plate.

Scenario 1		Scenario 2		Scenario 3		Scenario 4		Scenario 5	
Actual	Detected	Actual	Detected	Actual	Detected	Actual	Detected	Actual	Detected
0.2	0.20	0	-0.0	0	0.00	0.2	0.20	0	0.00
0.2	0.20	0.4	0.39	0.2	0.19	0.4	0.40	0.2	0.19
0.2	0.20	0.2	0.20	0.2	0.20	0.2	0.20	0.2	0.20
0	0.00	0.4	0.40	0	0.00	0	0.00	0.4	0.40
0	0.00	0	0.00	0.2	0.19	0	0.00	0	0.00
0.2	0.20	0.4	0.40	0	0.00	0	0.00	0.2	0.20
0.2	0.20	0	0.00	0.2	0.19	0	0.00	0.2	0.19
0	0.00	0	0.00	0	0.00	0	0.00	0.4	0.40
0	0.00	0.2	0.20	0	0.00	0.2	0.20	0.2	0.20
Scenario 6		Scenario 7		Scenario 8		Scenario 9		Scenario 10	
Actual	Detected	Actual	Detected	Actual	Detected	Actual	Detected	Actual	Detected
0.2	0.19	0	0.00	0.2	0.20	0	0.00	0.2	0.20
0	-0.0	0.2	0.19	0.2	0.20	0.4	0.40	0	0.00
0	0.00	0.2	0.20	0.2	0.20	0.2	0.20	0	0.00
0.2	0.19	0.4	0.40	0.2	0.20	0.4	0.40	0.2	0.19
0	0.00	0.2	0.20	0.2	0.20	0.2	0.19	0.2	0.20
0.2	0.20	0.2	0.20	0.4	0.40	0	0.00	0	0.00
0.2	0.19	0.2	0.20	0.2	0.20	0.2	0.20	0.2	0.19
0.2	0.20	0	0.00	0.2	0.20	0	0.00	0.2	0.20
0	0.00	0	0.00	0	0.00	0	0.00	0.2	0.20

3.3. Cantilever beam

For the steel beam considered, the material properties include Young's modulus E=200 GPa, mass density ρ=7850 kg/m3. The used cross-sectional is rectangular with width=2 cm and height=5 cm. Also, area and moment of inertia of the beam are A=0.001 m^2 and I=2.0833×10^{-7} m^4, respectively.

To investigate the effect of different short time loads on the proposed damage detection method, step load and two different rectangular loads have been used. The short time load excitations are applied at DOF=17 in *y* direction as shown in Figure 8 where F_0 = 2000 N and T_0 = 0.2 sec. For the cantilever beam, ten damage scenarios has been considered as seen in Table 7.

Time history displacement and velocity responses of cantilever beam in DOF=17 is shown in Fig. 9 for ten different damage scenarios. It can be seen that these responses are sensitive to structural damages and can be used as a damage indicator.

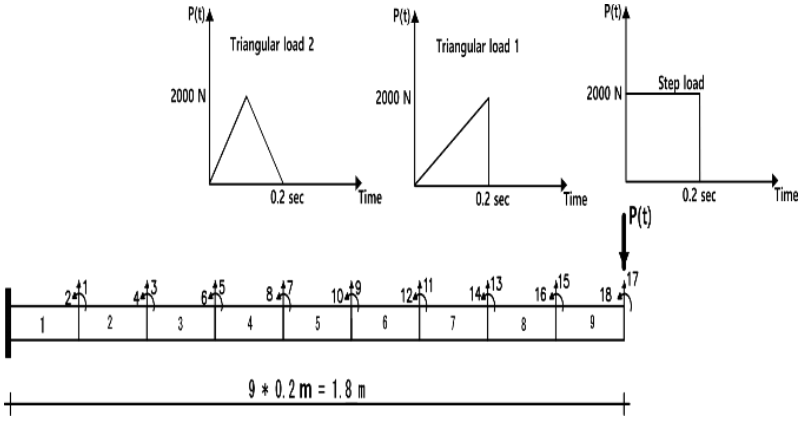

Fig. 8. Finite element model of the cantilever beam under three different short time loads.

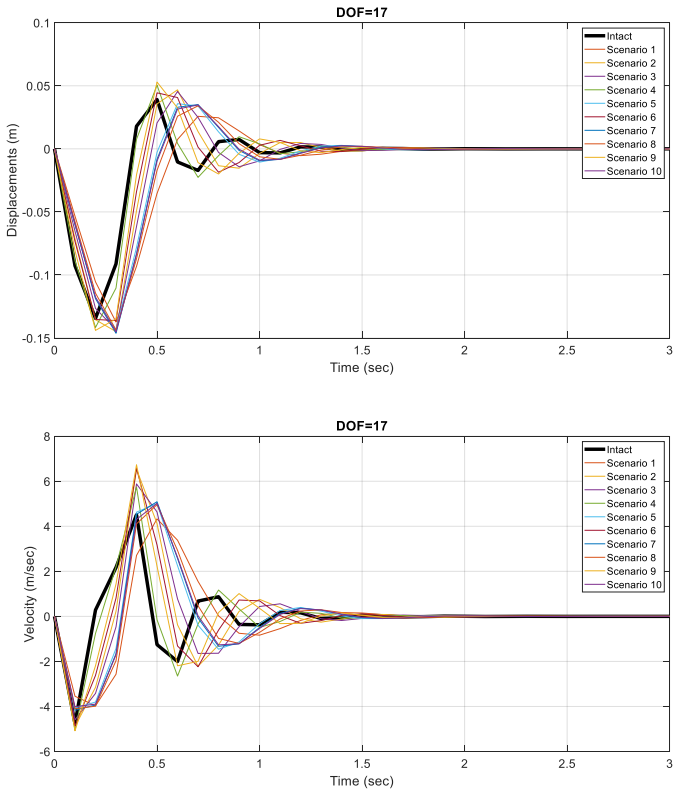

Fig. 9. Time history displacement and velocity responses of cantilever beam for step load.

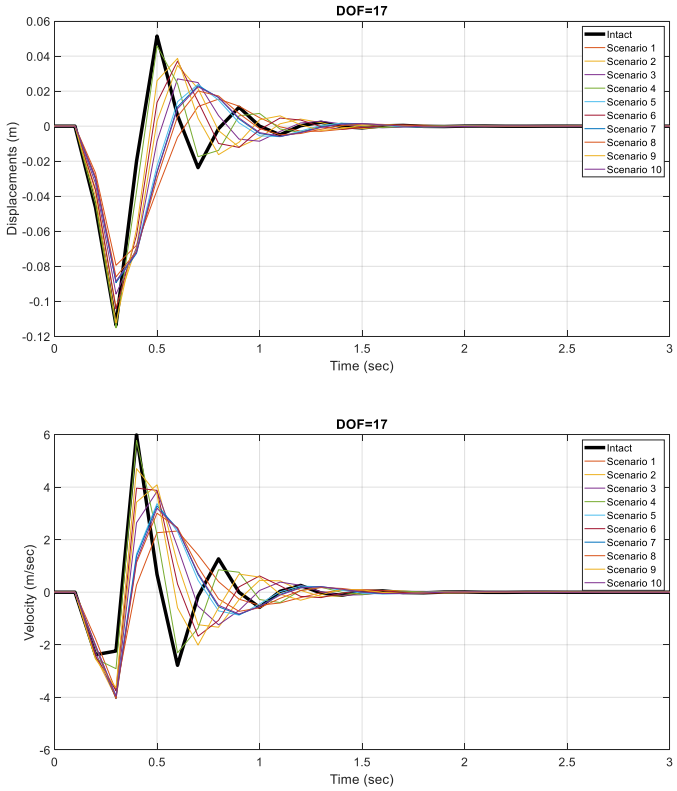

Fig. 10. Time history displacement and velocity responses of cantilever beam for triangular load 1.

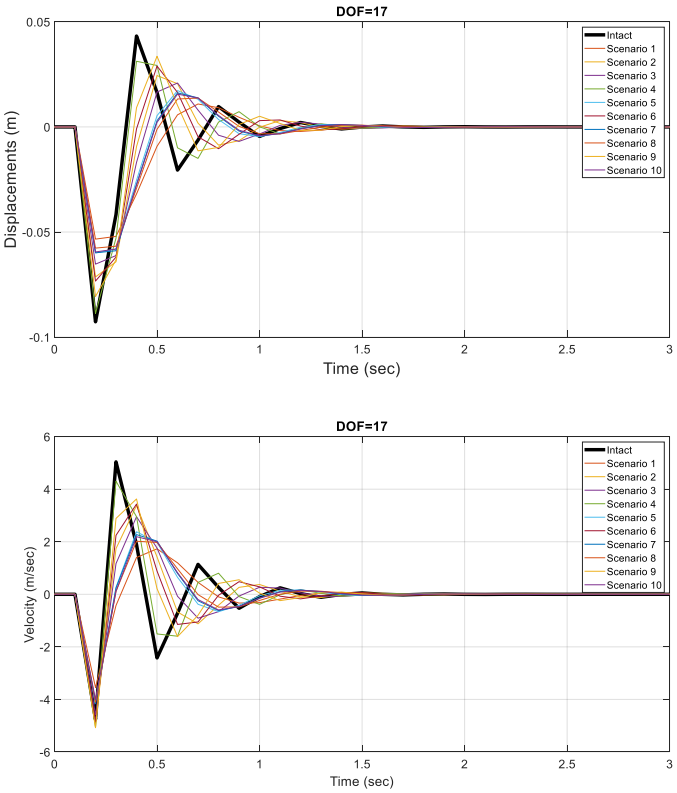

Fig. 11. Time history displacement and velocity responses of cantilever beam for triangular load 2.

The CFN performance in cantilever beam presented in Table 6. According to Table 6, the CFN trained accurately and can be used in damage identification process of cantilever beam.

Table 6. Statistics for training, validation and testing for beam under step load.

	Samples	MSE	R
Training	907	3.3e-4	0.9694
Validation	194	1.9e-3	0.9574
Testing	194	2.4e-3	0.9442

Table 7 show the detected damages for ten different scenarios in beam structure under step load. It can be seen that the proposed method can be used in damage detection process of cantilever beam. To investigate performance of presented method under different short time loads, two triangular loads applied as a different excitement. Tables 8 and 9 reveals that the presented method can identify damage accurately.

Table 7. The detected damages for ten different scenarios of beam under step load.

Scenario 1		Scenario 2		Scenario 3		Scenario 4		Scenario 5	
Actual	Detected	Actual	Detected	Actual	Detected	Actual	Detected	Actual	Detected
0.2	0.20	0.2	0.2	0.2	0.2	0	0.00	0.2	0.2
0.2	0.2	0.2	0.2	0.4	0.40	0.2	0.2	0	0.0
0	-0.0	0	0.0	0.2	0.2	0	0.0	0	0.01
0.2	0.19	0.2	0.18	0.4	0.4	0.2	0.19	0.2	0.2
0.2	0.17	0.2	0.19	0.2	0.2	0.2	0.19	0	0.01
0.2	0.18	0	-0.00	0.4	0.42	0.2	0.18	0.4	0.4
0	0.00	0	0.00	0.2	0.2	0	0.01	0.2	0.21
0.2	0.16	0	-0.0	0.4	0.39	0.2	0.2	0.4	0.4
0	0.04	0	0.05	0.2	0.16	0.2	0.13	0	0.03
Scenario 6		Scenario 7		Scenario 8		Scenario 9		Scenario 10	
Actual	Detected	Actual	Detected	Actual	Detected	Actual	Detected	Actual	Detected
0.2	0.2	0	0.00	0	0.00	0.2	0.2	0.2	0.20
0.2	0.21	0.2	0.21	0.4	0.41	0.2	0.19	0.4	0.41
0	0.01	0	-0.0	0	0.0	0.2	0.23	0.2	0.20
0.2	0.19	0.2	0.21	0	-0.03	0.4	0.4	0	0.00
0	0.0	0	0.02	0	-0.01	0.2	0.22	0	-0.01
0	0.00	0.4	0.38	0	0.00	0.4	0.41	0	0.00
0	0.0	0	-0.0	0.2	0.21	0.2	-0.21	0	-0.0
0.4	0.4	0.2	0.21	0	0.00	0.4	0.44	0.4	0.41
0.2	0.16	0.2	0.18	0	0.03	0	0.11	0	0.05

Table 8. The detected damages for ten different scenarios of beam under triangular load 1.

Scenario 1		Scenario 2		Scenario 3		Scenario 4		Scenario 5	
Actual	Detected	Actual	Detected	Actual	Detected	Actual	Detected	Actual	Detected
0.2	0.22	0.2	0.2	0.2	0.2	0	0.00	0.2	0.2
0.2	0.23	0.2	0.22	0.4	0.43	0.2	0.2	0	0.04
0	0.00	0	0	0.2	0.2	0	0.02	0	0.00
0.2	0.2	0.2	0.2	0.4	0.38	0.2	0.21	0.2	0.2
0.2	0.22	0.2	0.2	0.2	0.2	0.2	0.2	0	0.00
0.2	0.2	0	0.01	0.4	0.4	0.2	0.2	0.4	0.41
0	0.1	0	0.02	0.2	0.21	0	0.00	0.2	0.2
0.2	0.2	0	0.00	0.4	0.44	0.2	0.21	0.4	0.4
0	0.1	0	0.00	0.2	0.2	0.2	0.22	0	0.04
Scenario 6		Scenario 7		Scenario 8		Scenario 9		Scenario 10	
Actual	Detected	Actual	Detected	Actual	Detected	Actual	Detected	Actual	Detected
0.2	0.21	0	0.00	0	0	0.2	0.2	0.2	0.2
0.2	0.22	0.2	0.2	0.4	0.41	0.2	0.2	0.4	0.37
0	0.00	0	0.04	0	0.00	0.2	0.2	0.2	0.21
0.2	0.2	0.2	0.2	0	0.01	0.4	0.41	0	0.01
0	0.01	0	0.00	0	0.01	0.2	0.21	0	0.01
0	0.00	0.4	0.39	0	0.00	0.4	0.41	0	0.01
0	0.00	0	0.00	0.2	0.21	0.2	0.2	0	0.00
0.4	0.36	0.2	0.2	0	0.01	0.4	0.47	0.4	0.34
0.2	0.22	0.2	0.2	0	0.02	0	0.01	0	0.00

Table 9. The detected damages for ten different scenarios of beam under triangular load 2

Scenario 1		Scenario 2		Scenario 3		Scenario 4		Scenario 5	
Actual	Detected	Actual	Detected	Actual	Detected	Actual	Detected	Actual	Detected
0.2	0.22	0.2	0.22	0.2	0.24	0	0	0.2	0.2
0.2	0.23	0.2	0.24	0.4	0.4	0.2	0.26	0	0.00
0	0.00	0	0.00	0.2	0.2	0	0.00	0	0.01
0.2	0.20	0.2	0.20	0.4	0.4	0.2	0.2	0.2	0.24
0.2	0.20	0.2	0.2	0.2	0.2	0.2	0.2	0	0.00
0.2	0.20	0	0.00	0.4	0.44	0.2	0.2	0.4	0.34
0	0.00	0	0.01	0.2	0.2	0	0.00	0.2	0.21
0.2	0.20	0	0.00	0.4	0.46	0.2	0.21	0.4	0.41
0	0.01	0	0.03	0.2	0.2	0.2	0.22	0	0.00
Scenario 6		Scenario 7		Scenario 8		Scenario 9		Scenario 10	
Actual	Detected	Actual	Detected	Actual	Detected	Actual	Detected	Actual	Detected
0.2	0.21	0	0.00	0	0.00	0.2	0.18	0.2	0.2
0.2	0.23	0.2	0.2	0.4	0.38	0.2	0.2	0.4	0.39
0	0.01	0	0.00	0	0.00	0.2	0.2	0.2	0.2
0.2	0.2	0.2	0.2	0	0.04	0.4	0.38	0	0.00
0	0.00	0	0.00	0	0.01	0.2	0.2	0	0.00
0	0.01	0.4	0.41	0	0.02	0.4	0.41	0	0.00
0	0.00	0	0.00	0.2	0.18	0.2	0.2	0	0.00
0.4	0.39	0.2	0.21	0	0.00	0.4	0.39	0.4	0.44
0.2	0.2	0.2	0.22	0	0.00	0	0.00	0	0.01

4. Conclusion

In this paper a new damage identification procedure has been presented using time history response of different structure under short time load as an input to train cascade-forward network and damage states as output. Performance of presented method has been investigated using a plane frame, bending plate and cantilever beam. The mean-square error (MSE) and Correlation Coefficient (R) of the actual and detected damage severity values are determined. Also, trained CFN used to predict ten different damage scenarios.

In other part, to investigate performance of presented method under different short time loads, two triangular loads applied as a different excitement. Results reveal that the presented method is effective in damage identification of different structures.

Acknowledgments

This Work has been financially Supported by Azarbaijan Shahid Madani University Under the grant number 1884/1402.

References

[1] Bagheri A, Kourehli S. Damage detection of structures under earthquake excitation using discrete wavelet analysis 2013.

[2] Nouri Y, Shariatmadar H, Shahabian F. Nonlinearity detection using new signal analysis methods for global health monitoring. Sci Iran 2022. https://doi.org/10.24200/sci.2022.58196.5610.

[3] Nouri Y, Shahabian F, Shariatmadar H, Entezami A. Structural Damage Detection in the Wooden Bridge Using the Fourier Decomposition, Time Series Modeling and Machine Learning Methods. J Soft Comput Civ Eng 2024;8:83–101. https://doi.org/10.22115/scce.2023.401971.1669.

[4] Kourehli SS. Health monitoring of connections in steel frames using wavelet transform. Amirkabir J Civ Eng 2020;52:655–72.

[5] Jahangir H, Khatibinia M, Mokhtari Masinaei M. Damage detection in prestressed concrete slabs using wavelet analysis of vibration responses in the time domain. J Rehabil Civ Eng 2022;10:37–63.

[6] Beheshti Aval SB, Ahmadian V, Maldar M, Darvishan E. Damage detection of structures using signal processing and artificial neural networks. Adv Struct Eng 2020;23:884–97. https://doi.org/10.1177/1369433219886079.

[7] Roveri N, Carcaterra A. Damage detection in structures under traveling loads by Hilbert–Huang transform. Mech Syst Signal Process 2012;28:128–44. https://doi.org/10.1016/j.ymssp.2011.06.018.

[8] Yin T, Jiang Q-H, Yuen K-V. Vibration-based damage detection for structural connections using incomplete modal data by Bayesian approach and model reduction technique. Eng Struct 2017;132:260–77. https://doi.org/10.1016/j.engstruct.2016.11.035.

[9] Kourehli SS. Damage identification of structures using second-order approximation of Neumann series expansion. J Rehabil Civ Eng 2020;8:81–91.

[10] Katkhuda H, Shatarat N, Hyari K. Damage detection in steel structures with semi-rigid connections using unscented Kalman filter. Int J Struct Integr 2017;8:222–39. https://doi.org/10.1108/IJSI-04-2016-0014.

[11] Zimin VD, Zimmerman DC. Structural Damage Detection Using Time Domain Periodogram Analysis. Struct Heal Monit 2009;8:125–35. https://doi.org/10.1177/1475921708094796.

[12] Kourehli SS. Gaussian Process Regression Model for Damage Localization in Plates Based on Modal Data. J Rehabil Civ Eng 2022;10:68–78.

[13] Seyedpoor SM, Ahmadi A, Pahnabi N. Structural damage detection using time domain responses and an optimization method. Inverse Probl Sci Eng 2019;27:669–88. https://doi.org/10.1080/17415977.2018.1505884.

[14] Ogata K. Modern control engineering. B Rev 1999;35:1184.

[15] Mendoza Zabala JL. State-space formulation for structure dynamics 1996.

[16] MATLAB Documentation 2022.

[17] Warsito B, Santoso R, Suparti, Yasin H. Cascade Forward Neural Network for Time Series Prediction. J Phys Conf Ser 2018;1025:012097. https://doi.org/10.1088/1742-6596/1025/1/012097.